NASA TECHNICAL NOTE

NASA TN D-6464

ENERGY DEPENDENCE OF ELECTRON-INDUCED RADIATION DAMAGE IN TUNGSTEN

by James A. DiCarlo and James T. Stanley

Lewis Research Center
Cleveland, Ohio 44135

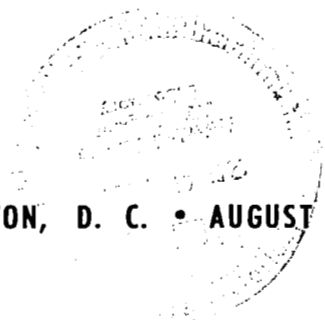

NATIONAL AERONAUTICS AND SPACE ADMINISTRATION • WASHINGTON, D. C. • AUGUST 1971

1. Report No.	2. Government Accession No.
NASA TN D-6464	

4. Title and Subtitle	5. Report Date
ENERGY DEPENDENCE OF ELECTRON-INDUCED RADIATION DAMAGE IN TUNGSTEN	August 1971
	6. Performing Organization Code

7. Author(s)	8. Performing Organization Report No.
James A. DiCarlo and James T. Stanley	E-6330
	10. Work Unit No. 129-03

9. Performing Organization Name and Address	11. Contract or Grant No.
Lewis Research Center National Aeronautics and Space Administration Cleveland, Ohio 44135	
	13. Type of Report and Period Covered Technical Note

12. Sponsoring Agency Name and Address	14. Sponsoring Agency Code
National Aeronautics and Space Administration Washington, D.C. 20546	

15. Supplementary Notes

16. Abstract

The onset and low dose "effective" threshold energies for the 350 K production of electron-induced damage in tungsten were determined to be 50±2 eV and 52±2 eV, respectively (electron energy = 1.62 MeV). These results when combined with bcc damage theory and other experimental data suggest (1) the 350 K thresholds should hold from 100 to 600 K, (2) the minimum recoil energy required for "free" interstitial production near 0 K is 53±5 eV, (3) threshold in tungsten has little dependence on crystal direction, and (4) threshold in any bcc transition metal can be estimated by assuming a direct proportionality with Young's modulus.

17. Key Words (Suggested by Author(s))	18. Distribution Statement
Tungsten Electron irradiation Threshold energy for displacement Radiation damage	Unclassified - unlimited

19. Security Classif. (of this report)	20. Security Classif. (of this page)	21. No. of Pages	22. Price*
Unclassified	Unclassified	27	$3.00

*For sale by the National Technical Information Service, Springfield, Virginia 22151

ENERGY DEPENDENCE OF ELECTRON-INDUCED RADIATION DAMAGE IN TUNGSTEN

by James A. DiCarlo and James T. Stanley*

Lewis Research Center

SUMMARY

The energy dependence of low dose damage production in commercial and high purity polycrystalline tungsten wires was studied near 350 K with 1.6 to 2.4 MeV electrons. From resistivity measurements at 291 K the threshold energy for the onset of observable damage was determined as 50±2 eV. An "effective" threshold of 52±2 eV was also determined by directly fitting the energy dependence of the damage rates to theoretical displacement cross sections calculated from step-function displacement probabilities. A decrease of two orders of magnitude in impurity content reduced damage rates by about a factor of two but did not affect threshold. These results combined with current defect recovery models for tungsten, low temperature threshold data, and computer-calculated bcc damage theory suggest: (1) Observed damage consisted of equal concentrations of vacancies and impurity-trapped Stage I free interstitials. (2) Across Stage II (100 to 600 K) onset threshold should be within 50±2 eV. (3) Minimum recoil energy required for free interstitial production near 0 K is 53±5 eV. (4) Threshold has little dependence on crystal direction.

An empirical method is presented for predicting threshold energies in the bcc transition metals by assuming the directional dependence of threshold is directly proportional to that of Young's modulus. By the use of one universal proportionality constant (1.2×10^{-6} (eV)(cm^2)/N), thresholds for a number of metals and directions are calculated and shown to have significantly better agreement with experiment than the best available theoretical estimates.

*Associate Professor of Engineering, Arizona State University, Tempe, Arizona.

INTRODUCTION

The present study was undertaken to determine the effects of a Stage II irradiation temperature on the threshold energy for displacement and the production of electron-induced damage in tungsten. Stage II for tungsten is that defect recovery stage from 100 to 600 K which has been attributed to the release of impurity-trapped interstitials that first become mobile during Stage I (refs. 1 and 2). Although only a fraction of the total damage is retained, irradiations within Stage II can provide useful information concerning the effects of temperature and purity on the threshold energy and the damage rate. From these results further information might then be deduced concerning the recoil energy required for free interstitial production and the dependence of threshold energy on recoil direction. The Stage II irradiations of the present work were performed at ~350 K not only for experimental convenience but also because the knowledge obtained near room temperature is more technically useful than that obtained at lower temperatures.

THEORY

The threshold energy for displacement E_d is the minimum recoil energy which an atom in a perfect lattice must receive in order to produce an atomic displacement. The simplest manner in which it can be determined is by measuring the electron energy ϵ_d^o at which the first observable irradiation-induced damage is produced. Then, from energy transfer considerations, the threshold energy for the onset of damage E_d^o is given by

$$E_d^o = E_r^{max}(\epsilon_d^o) \tag{1}$$

where

$$E_r^{max}(\epsilon) = \frac{2(\epsilon + 2mc^2)}{Mc^2}\epsilon \tag{2}$$

Here E_r^{max} is the maximum recoil energy that the struck atom can receive from an electron of energy ϵ, and mc^2 and Mc^2 are the rest mass energy of the electron and atom, respectively.

At irradiation temperatures within the lower portion of Stage I, there are situations when the damage onset method cannot be employed for an accurate threshold determination. This is due primarily to the existence of subthreshold displacements caused by extrinsic sources (ref. 3). In these situations the usual approach is to assume that the

probability for displacement $P(E_r)$ is a step function, that is, $P = 0$ for $E_r < E_d^*$ and $P = 1$ for $E_r \geq E_d^*$. The "effective" threshold energy E_d^* can then be determined by measuring the energy dependence of the damage rate and finding the "best" theoretical displacement cross section which obeys the relation

$$\frac{d\rho}{d\Phi}(\epsilon) = \rho_F \sigma_d(\epsilon, E_d^*) \tag{3}$$

where $d\rho/d\Phi$, the damage rate, is the change in specimen resistivity ρ per unit change in electron dose Φ; ρ_F is the specific resistivity per interstitial-vacancy (Frenkel) pair; and $\sigma_d(\epsilon, E_d^*)$ is the displacement cross section calculated from a step function $P(E_r)$. Here it is assumed that all displaced atoms are retained and observed and that ρ_F is independent of interstitial-vacancy separation. For many metals in which both thresholds have been determined, E_d^* has been found to be equal to or slightly larger than E_d^o by only a few electron volts (ref. 3).

Because equation (3) assumes the retention of all damage, it cannot describe the energy and dose dependence of the damage rate for irradiation temperatures above Stage I defect recovery. The proper Stage II relation which has had experimental verification (refs. 4 and 5) was originally given by Walker (ref. 6); namely,

$$\left[\frac{d\rho}{d\Phi}(\epsilon)\right]_{II} = \frac{f(\epsilon)\rho^* \sigma_d(\epsilon, E_d^*)}{\left(1 + \frac{2\sigma_d \Phi}{N_u}\right)^{1/2}} \tag{4}$$

Here $f(\epsilon)$ is the fraction of displaced atoms or interstitials created far enough from their own vacancies to be uncorrelated; ρ^* is the resistivity per Frenkel pair when the interstitial member is trapped at an impurity atom; and N_u is the total concentration of impurity atoms capable of capturing interstitials at the irradiation temperature. These impurity atoms are considered to be "unsaturable"; that is, their trapping efficiency is unaltered after capturing one or more interstitials.

The right side of equation (4) can be understood as the product of three probabilities: the probability per unit dose of producing a displaced atom - $\sigma_d(\epsilon, E_d^*)$; the probability that this displacement is an uncorrelated interstitial - $f(\epsilon)$; and the probability that this interstitial will be captured by an unsaturable trap before encountering a vacancy - $\left[1 + (2\sigma_d \Phi / N_u)\right]^{-1/2}$. The physical basis for the latter two probabilities centers on the model that at a Stage II temperature all irradiation-induced interstitials have sufficient thermal energy to migrate immediately after creation. Most perform correlated motion toward their own vacancies where they disappear from experimental detection. However, a certain fraction f of the interstitials are uncorrelated or "free" interstitial atoms

(FIA) which, because they wander randomly in the lattice, can be trapped by an impurity before encountering a vacancy. Thus the impurities retain the FIA and their vacancies for observation. Walker assumes that the probability for FIA to be trapped is given by $N_u/(N_u + v)$ where v is the total vacancy concentration at the time the FIA are wandering around the lattice. Initially $N_u >> v$ so that essentially no FIA reach vacancies and resistivity increases linearly with dose. As v increases, however, more and more FIA reach and annihilate vacancies before becoming trapped, resulting in an observable reduction in $d\rho/d\Phi$. Eventually $v >> N_u$ and $d\rho/d\Phi = 0$. Since $v \cong \sigma_d \Phi$, competition between v and N_u for FIA capture is contained mathematically in the denominator of equation (4).

Determination of E_d^* with equation (4) is complicated by the parameters N_u and f. To minimize their effects, the following simplifications were employed in the present study. First, because N_u could not be accurately estimated, damage rates were measured only in the low dose region where $N_u >> v$ and $d\rho/d\Phi$ is independent of Φ. Under these conditions equation (4) reduces to

$$\left[\frac{d\rho}{d\Phi}(\epsilon)\right]_{II} = f(\epsilon)\rho^* \sigma_d(\epsilon, E_d^*) \tag{5}$$

Secondly, because $f(\epsilon)$ should increase with energy in an unknown manner, the approach taken here is to define E_d^* for Stage II as that effective threshold energy which satisfies equation (5) under the assumption that $f(\epsilon) = f_o = \text{constant}$. That is, for a Stage II irradiation temperature T, the damage rate is considered to be directly proportional to the displacement cross section so that $E_d^*(T)$ can be determined by the same methods discussed with equation (3). It should be pointed out that the E_d^* calculated in this manner may differ from the value calculated with the full theory (eq. (4)). However, as the experimental results will show, this approach does yield an $E_d^*(T)$ essentially equal to $E_d^o(T)$ and thus, at least for tungsten, is another and perhaps more convenient method for determining the Stage II threshold energy for displacement.

EXPERIMENTAL PROCEDURE

The specimens primarily employed for the threshold determinations were commercial purity 2-mil-diameter polycrystalline wires supplied by General Electric. Resistivity ratio measurements yielded values of about 10, indicating a purity of ~99.5 percent for this material (ref. 7). A high purity 5-mil-diameter polycrystalline wire was used to check both the commercial purity results and previous low temperature data; that is, the high purity wire was identical to that employed by DiCarlo, Snead, and Goland (ref. 8)

for radiation damage studies near 20 K. The residual resistivity ratio of this wire was estimated to be greater than 1000, indicating a purity of ~99.995 percent and thus an impurity concentration some two orders of magnitude smaller than the commercial wire.

Resistivity changes caused by the electron damage were measured at 291 K using a specimen and dummy in a standard bridge circuit to eliminate thermal effects. Each wire was held at one end by a copper clamp and at the other end by a mica-insulated clamp, resulting in an exposed length of about 1.2 centimeters. Voltage probes consisted of 1-mil tungsten wires spot-welded 1 centimeter apart. Because the ratio of measurement length to cross-sectional area could not be made identical for the two wires, there existed the possibility of a slight thermal resistivity error if consecutive measurements were not made at exactly the same temperature. This type of error was minimized in two ways. First, the preirradiation currents through the specimen and dummy were separately adjusted until the voltage drops across each wire were identical. Theoretically it can be shown that if these preirradiation currents were maintained during subsequent measurements, errors due to nonrepetitive temperatures should not exist. Experimentally, however, this method was not completely adequate since resistivity deviations could be observed if the temperature variations were allowed to exceed 1 K. Therefore a temperature controller was introduced to repeat temperatures to within ±0.2 K as measured by a Chromel-Alumel thermocouple. The controller, a PAR model 152, balanced the input current to heaters within the specimen holder against the cooling power of a thermoelectric cooler. Resistivity and current ratio measurements were made using a 6-dial Rubicon double potentiometer with a voltage resolution of 0.01 microvolt. Since the currents through the 2- and 5-mil specimens were maintained at 40 and 100 milliamperes, respectively, the total measurement system had a resolution on the order of 10^{-11} ohm-centimeter in defect resistivity.

Electron irradiations were performed in the vacuum of the Lewis Dynamitron accelerator. Near beam uniformity was achieved by magnetically expanding the beam and allowing about 10 percent or less of its center portion to pass through an aperature immediately in front of the specimen. The consistency of this uniformity was continually checked by monitoring the specimen's voltage rise under identical beam current conditions. It was determined both theoretically and experimentally that beam heating caused the specimens to rise to an average temperature of about 350 K. This temperature was produced by an operating beam current density of ~50 microamperes per square centimeter measured by a Faraday cup directly behind the specimens. Systematic and random errors in the integrated dose measurements were estimated at less than 5 and 1 percent, respectively.

Electron energy was measured by the divider-board current of the Lewis Dynamitron accelerator and the 1968 calibration results of Stevenson and Gauntner (ref. 9). A $Be(\gamma,n)$ calibration at 1.662 MeV indicated that since this latter study the resistance of

the divider board had not changed more than 0.1 percent (~1.7 keV). From a consideration of this result and other possible sources of error, each energy measurement of the present study was estimated to have a total absolute error less than 10 keV.

For an accurate determination of damage rate, the measured values of $d\rho/d\Phi$ had to be corrected for two energy-dependent deviations caused by the finite diameter of the wire specimens. First, due to electron energy losses within the wires, the displacement cross section decreases with depth into the material, giving rise to position-dependent resistivity changes. According to Sosin (ref. 10), this energy loss effect can be averaged by assuming that the resistivity was measured at an average electron energy $\bar{\epsilon}$ given by

$$\bar{\epsilon} = \epsilon_i - \frac{4}{3\pi} \alpha d \tag{6}$$

where ϵ_i is the incident electron energy, α is the specific energy loss per unit distance, and d is the diameter of each wire. In the present work the α's calculated by Berger and Seltzer (ref. 11) were employed.

The second energy-dependent correction is required because the electrons undergo multiple scatterings within each specimen, resulting in an average electron path length greater than the specimen thickness parallel to the beam direction. Because an increased path length implies a larger effective electron flux dependent on energy and position, the measured resistivity damage rate $(d\rho/d\Phi)_m$ is an energy- and thickness-dependent fraction of $(d\rho/d\Phi)_0$, the "true" or zero diameter damage rate. Again according to Sosin (ref. 10),

$$\left(\frac{d\rho}{d\Phi}\right)_0 = \left(\frac{d\rho}{d\Phi}\right)_m \left(1 + \frac{\pi a d}{4}\right)^{-1} \tag{7}$$

The parameter a can be determined from the average path length increase Δ in a foil of thickness t; that is,

$$a = \frac{\Delta(t)}{t^2}$$

As discussed by Oen (ref. 12) there has been some question as to the correct theoretical expression for Δ, often referred to as the Yang correction. Following Oen's suggestion the present work employs the following relation for a:

$$a = \frac{\Delta(\bar{t})}{\bar{t}^2} = \frac{\left[\theta_w(\bar{t})\right]^2}{4\bar{t}} \tag{8}$$

where $\bar{t}$ (= $\pi d/4$) is the average thickness of each wire and θ_w is the empirically corrected mean scattering angle contained in Moliere multiple scattering theory (ref. 13).

EXPERIMENTAL RESULTS

The general measurement procedure for determining damage rate as a function of energy was as follows. Because preirradiation handling may have introduced defects which anneal at the irradiation temperatures (ref. 7), each specimen was initially beam-annealed for a few minutes at an average temperature of ~420 K. After the anneal, the specimen was irradiated at constant energy until linearity of the resistivity production curve was established and an accurate value of the slope could be determined. A new energy was then chosen and the same specimen was reirradiated without any intervening anneal. After slope measurement the aforementioned process was repeated until the total irradiation-induced resistivity reached an arbitrary value of $\sim 10^{-8}$ ohm-centimeter ($\sim 2\times10^{-5}$ defect concentration). Typical resistivity production curves are given in figure 1 for one of the commercial specimens. Table I lists the slope and standard deviation of each production curve at the incident energy ϵ_i and the corresponding maximum recoil energy E_r^{max} given by equation (2). The deviations in slope were attributed primarily to slight variations in beam uniformity, except for the first commercial specimen where no temperature controller was employed.

From table I it can be seen that 350 K radiation damage in tungsten does not measurably commence in the commercial wires until electrons attain an energy somewhere between 1.58 and ~1.66 MeV. This latter value was inferred from a worst case extrapolation of the finite damage rate measured at 1.70±0.01 MeV. Therefore, using equations (1) and (2) one can conclude that near 350 K the onset threshold energy for displacement in tungsten lies between 48 and 52 eV; that is, $E_d^o(350\ K) = 50\pm2$ eV.

In order to compute the effective threshold energy, the energy loss and path length corrections given by equations (6) to (8) were applied to the data of table I. The results are plotted in figure 2. The commercial data points are indicated by open blocks and the limited high purity data by solid blocks. From equation (5) and the tabulated displacement cross section data of Burke, Grossbard, and Lowe (ref. 14), it was determined that the best fit $\sigma_d(\epsilon, E_d^*)$ for the commercial results gave $E_d^*(350\ K) = 52\pm2$ eV and $f_o\rho^* = (2.1\pm0.4)\times10^{-4}$ ohm-centimeter. The energy dependence of the product $f_o\rho^*\sigma_d(\epsilon, 52\ eV)$ is shown by the solid line of figure 2. The best fit cross sections were

determined only with the data above 1.9 MeV since deviations in threshold energy due to lattice structure, subthreshold displacements, and specimen thickness may be present in the near-threshold data (ref. 3). However, as can be seen, the σ_d based on a 52-eV step function fits nearly all the low energy data. Thus, even for irradiation temperatures above Stage I, the threshold determination method which assumes the (low dose) damage rate to be directly proportional to a theoretical $\sigma_d(E_d^*)$ can yield an $E_d^*(T)$ essentially equal to $E_d^o(T)$.

As shown by the dashed line of figure 2, the best fit curve for the high purity damage rates yields $E_d^* = 54$ eV and $f_o\rho^* = 1.3\times10^{-4}$ ohm-centimeter. Although agreement with the commercial threshold is good, the fact that there are only two points makes any E_d^* assignment for this material somewhat tenuous. Also, the validity of applying the path length correction to the high purity data is questionable since θ_w for 5-mil tungsten ($\sim60^o$) is well above the maximum Moliere scattering angle (30^o). However, assuming that only the magnitude and not the energy dependence of the path length correction was in error, it was determined that doubling or even eliminating the correction has negligible effect on E_d^* for either specimen type but only alters $f_o\rho^*$. It should also be pointed out that, no matter what its absolute value may be, the path length correction should have a greater reducing effect on the measured damage rates of the larger diameter high purity specimen than on the measured rates of the commercial specimens. Thus the smaller table I damage rates for the high purity specimen are real and cannot be accounted for by the path length correction.

DISCUSSION

The threshold energy and damage rate results of the present study have both basic and applied implications which can only be appreciated in the light of radiation damage theory and other experimental data. For instance, by comparing the 350 K threshold energies with similar low temperature results, one may obtain fundamental knowledge concerning the effects of temperature, recoil energy, and recoil direction on the production and deposition of damage. Although this knowledge would primarily concern tungsten, inferences for other bcc metals can result. In addition, there is the practical aspect of the damage rate results, namely, the capability of estimating total irradiation-induced defect concentrations when tungsten of a certain purity is subjected to electron bombardment at Stage II temperatures. The discussion that follows will consider each of the aforementioned topics in more detail.

THRESHOLD IN TUNGSTEN

Theoretical Effects of Temperature

Before discussing the experimental temperature dependence of threshold in tungsten, one should first consider the possible theoretical effects of temperature on the displacement and retention of an atom in a real crystal. The many aspects of this subject have been adequately covered in a recent review article by Sosin and Bauer (ref. 3). Hence we will briefly re-examine only that theory pertinent to the present experiment, concentrating on such topics as displacement theory with and without thermal vibration and the mechanisms currently invoked for low temperature defect recovery in tungsten.

Displacement theory. - Consider defect production in a perfect lattice at 0 K. Because the structure surrounding each atom in the lattice is discrete, the threshold energy for displacement E_d is a function of the atom's initial recoil direction; that is, $E_d = E_d\langle hk\ell \rangle$ where the indices h, k, and ℓ describe the recoil direction in terms of the principal crystal axes. Since $E_d^o(0\ K)$ is the minimum recoil energy required to produce a displacement, it follows that $E_d\langle hk\ell \rangle \geq E_d^o(0\ K)$. Computer studies on both fcc (ref. 15) and bcc (ref. 16) lattices have found that in contrast to the vacancy the interstitial is not created at the collision site but is usually the result of a replacement collision chain. That is, the initial recoil atom first displaces one of its neighbors by transferring a large fraction of E_r and then replaces this neighbor in its original position. This sequence of energy transfer and replacement continues from neighbor to neighbor until a collision occurs in which the energy transferred is insufficient to displace an atom from its original site. The energy loss per replacement was found to vary with crystal direction of the chain, being smallest for the closest-packed direction. Thus the final outcome of the electron collision is an atom in an interstitial position separated from a vacant lattice site by a distance which is dependent on the initial recoil energy, the initial recoil direction, and the crystal direction in which the replacement chain occurred.

If E_r^{max}, the maximum recoil energy available from the incident electrons (eq. (2)), equals $E_d^o(0\ K)$, the interstitial will be created as close to the vacancy as possible without recombining. Therefore $E_d^o(0\ K)$ is the threshold energy required for the production of a Frenkel pair characterized by minimum separation between the vacancy and the "close-pair" interstitial atom (CPIA). On the average this close-pair separation should increase with $E_r^{max} - E_d^o(0\ K)$. Eventually at some E_r^{max} equal to $E_d(FIA)$ a few interstitials will attain a separation large enough to be outside the attractive influence of their own vacancies, thereby becoming uncorrelated or FIA.

Introducing thermal vibration into a perfect lattice can affect the two basic aspects of damage production, that is, the displacement of the initial recoil atom and the retention of the resulting interstitial. For example, temperature can alter the displacement

process by contributing thermal momentum to the collision momentum of the recoil atom, thereby lowering the onset threshold energy (ref. 3). If the collision and thermal momentum happen to be parallel at impact, then

$$E_d^o(T) \cong E_d^o(0\ K) - 2\left(E_d^o E_v\right)^{1/2} \tag{9}$$

where $E_v = kT$ is the thermal energy of the struck atom. For $E_d^o \cong 50$ eV and $T = 350$ K, $E_d^o(0\ K) - E_d^o(T) \cong 2.5$ eV. If the thermal momentum of the atoms surrounding the struck atom happen to be 180^o out of phase with that of the atom, another 2.5 eV energy gain may result. Thus, due to this temperature-enhanced displacement effect (TEDE), E_d^o measured at 350 K in tungsten may be as much as 5 eV lower than that measured near 0 K. However, E_d^* should be unaffected by TEDE since it is determined from damage rates measured at $E_r^{max} > E_d^o$. That is, to first order the average contribution of all thermal momentum directions to these damage rates is zero.

Another effect that temperature may have on threshold energy concerns the problem of damage retention. Whenever thermal vibrations exist, there is a finite probability that the irradiation-induced interstitials will gain sufficient thermal energy to migrate from one lattice position to another until a vacancy is encountered and both defects are annihilated. Because of strain considerations, the activation energy and thus the temperature required for this migration should increase with interstitial-vacancy separation, being smallest for those CPIA nearest their vacancies and largest for the FIA. Indeed, extensive low temperature irradiation studies on copper and other metals (ref. 17) have found that this model adequately explains the variety and behavior of the damage recovery peaks observed during annealing through Stage I, the temperature region containing initial damage recovery. That is, as temperature is increased within Stage I, CPIA with larger activation energies for migration gain sufficient thermal energy to perform correlated motion toward their own nearby vacancies (first-order kinetics); until at the end of Stage I the uncorrelated FIA wander freely throughout the lattice, encountering vacancies in a random fashion (second-order kinetics). Therefore, although both CPIA and FIA can be created at any irradiation temperature T, only those interstitials whose characteristic recovery temperatures are above T will be retained in the specimen to be measured. The only exception is the FIA which because of its random migration has a finite probability of being impurity-trapped and thereby retained above its intrinsic recovery temperature T_{FIA}. Generally Stage II, the next higher temperature region above T_{FIA}, has been found to encompass those recovery peaks associated with FIA release from impurity traps. Therefore, if greater onset thresholds for larger interstitial-vacancy separations are assumed and TEDE is neglected, it follows that $E_d^o(T)$ should increase with increasing irradiation temperature within Stage I, reaching at T_{FIA} the value $E_d(FIA)$ which should remain constant throughout Stage II. However, E_d^* as

determined with the full Stage II theory should be unaffected by the damage retention problem because, as explained with equation (4), the retention aspect is explicity contained in the probabilities $f(\epsilon)$ and $\left[1 - (2\sigma_d\Phi/N_u)\right]^{-1/2}$ and not in the displacement probability $\sigma_d(\epsilon, E_d^*)$.

In summary, the possible theoretical effects of a 350 K Stage II irradiation on threshold energy in tungsten are as follows. Onset threshold may or may not be larger than E_d^o(0 K); that is,

$$E_d^o(350\ \text{K}) = E_d^o(0\ \text{K}) + \Delta E_{FIA} - (2.5 \pm 2.5) = E_d(\text{FIA}) - (2.5 \pm 2.5) \qquad (10)$$

Here ΔE_{FIA} is the difference in recoil energy required to create an FIA and that required to create a Frenkel pair with minimum defect separation. The last term in parentheses is the average contribution (eV) at 350 K of the TEDE. On the other hand, the effective threshold E_d^* as determined with the full theory (eq. (4)) should have the same value at any irradiation temperature within Stage II as that determined near 0 K (eq. (3)).

Defect recovery in tungsten. - From the previous discussion it is obvious that proper analysis of the temperature dependence of threshold in tungsten depends on a knowledge of the temperature regions during which CPIA and FIA migrate and impurity-trapped interstitials are released. The initial resistivity recovery measurements on fast-neutron-irradiated tungsten by Kinchin and Thompson (ref. 18) have shown the existence of three low temperature recovery stages: Stage I, 0 to 100 K; Stage II, 100 to 600 K; and Stage III, 600 to 750 K. Thompson (ref. 1) suggested that Stage I recovery be assigned to interstitial motion, Stage II to the release of impurity-trapped interstitials, and Stage III to vacancy motion. Since then, further radiation damage experiments on tungsten have found general agreement with these assignments.

Within Stage I, for example, the many recovery peaks observed by Coltman, Klabunde, and Redman (ref. 19) after thermal neutron irradiation are suggestive of the recombination of a variety of close Frenkel pairs each with different interstitial-vacancy separation. Regarding the location of T_{FIA}, DiCarlo, Snead, and Goland (ref. 8) found that in electron-irradiated tungsten more damage recovered between 45 and 100 K after the specimen was predoped with excess vacancies. Such behavior would be expected if FIA move in this temperature range because the larger vacancy concentration should increase the probability that the FIA will be vacancy annihilated rather than impurity trapped. Neely, Keefer, and Sosin (ref. 20) have shown that recovery near 70 K in electron-irradiated tungsten followed second-order kinetics, a result which suggests FIA migration to vacancies near this temperature. More recently Scanlan, Styris, and Seidman (refs. 21 and 22) have performed a careful field ion microscope study with very high purity tungsten irradiated from 8 to 15 K with 20-keV tungsten ions. In the presence of the best imaging electric field they observed FIA reaching the specimen's surface

beginning at ~28 K and peaking at ~38 K. Because this surface field produced a large tensile stress within the bulk material, they were unable to conclude whether their FIA annealing temperatures represented T_{FIA} in a stress-free tungsten specimen. However, they do point out that if the activation volume for FIA migration in tungsten were similar to that calculated by Johnson (ref. 23) for the ⟨110⟩ split FIA in α-iron (+0.1 atomic volume), then T_{FIA} in stress-free tungsten should occur near the 70 K recovery peak observed by Neely, Keefer, and Sosin.

Support for the release of impurity-trapped interstitials in Stage II has been found by DiCarlo and Townsend (ref. 2) who observed internal friction peaks near 100 and 200 K in deuteron-irradiated tungsten. These peaks existed only in impure samples and were traceable to the stress-induced ordering of interstitial-impurity complexes. Regarding the mechanism responsible for Stage III recovery, there exists some evidence (ref. 24) that a second form of the interstitial is annealing in this stage and that vacancy motion should be assigned to higher temperatures. Because the present results do not apparently give preference to either of these proposed mechanisms, we will not pursue this Stage III question further but only emphasize the generally accepted fact that tungsten vacancies do not migrate until at least 600 K or well above the maximum temperatures achieved here.

Experimental Effects of Temperature

Although there have been a number of low temperature radiation damage studies in tungsten, only two have yielded threshold values with accuracies comparable to that obtained here. Roberts (ref. 25) using electron irradiation at ~35 K measured damage rates near E_d^o. Although he did not reach energies where no damage was observed, he was able to extrapolate his data to the zero damage point, obtaining $E_d^o(35\ K) = 47 \pm 3$ eV. Also, Neely, Keefer, and Sosin (ref. 20) measured electron-induced damage rates at three energies near 4 K, from which they estimate $E_d^o(4\ K) = 40 \pm 2$ eV.

No previous experiment has determined a low temperature E_d^* for tungsten. Nevertheless there seems to be sufficient published damage rate as a function of energy data to arrive at an approximate value for the effective threshold. For example, one can obtain the four data points shown in figure 3 from the 4 K damage rates of Neely, Keefer, and Sosin (ref. 20) and the 20 K rate of DiCarlo, Snead, and Goland (ref. 8) after correction for energy loss (eq. (6)) and path length (eqs. (7) and (8)). It should be emphasized that there can be significant deviations in electron dose measurements from laboratory to laboratory. In addition the 20 K point was probably observed above the annealing temperatures of some CPIA implying that, if the irradiation were performed near 4 K, a

larger damage rate would have been measured. To account for this latter problem we show by an arrow in figure 3 that this point could be higher near 4 K. Assuming a few values for this point and neglecting dose errors, we have fitted the three high energy damage rates to the theoretical displacement cross sections of Burke, Grosshard, and Lowe (ref. 14). The lowest energy damage rate was omitted because of the possibility of subthreshold displacements. We thus obtain the curves in figure 3, indicating $E_d^* \geq 46$ eV and $\rho_F \geq 4.1 \times 10^{-6}$ ohm-centimeter per atomic percent of Frenkel pairs. This latter result can be compared with the value determined by Schultz (ref. 7) of 2.5×10^{-6} ohm-centimeter per atomic percent of tungsten vacancies.

A summary of all results concerning the temperature dependence of threshold energy in tungsten is given in table II. The defect recovery model which puts T_{FIA} near 70 K has been employed to label E_d^o(35 K) as a Stage I measurement. As previously explained with equation (5), the Stage II E_d^*(350 K) may be in error due to the fact that it was determined under the assumption that $f(\epsilon)$ was independent of energy. However, since E_d^* should be unaffected by temperature, the correct 350 K value which would have resulted from employing the full theory (eq. (4)) should be that determined near 4K. Thus it can be seen from table II that the assumption of constant f produced only a small error, if any, on the determination of E_d^* for tungsten.

The majority of the data in table II indicates that across Stage I and a large portion of Stage II threshold energy in tungsten is nearly independent of temperature. The only exception appears to be the E_d^o(4 K) result which is derived from the lowest energy point of figure 3. The fact that this point does not fall on the best cross section lines can be explained either by a large anistropy in $E_d\langle hk\ell \rangle$ or by the existence of subthreshold displacements. For instance, if the threshold in one crystal direction is lower than the average threshold for all directions, then near threshold a small amount of damage due to displacements in that specific direction will be observed; whereas at the higher energies the average threshold is exceeded and the damage is caused by displacements in essentially all directions. Or, the presence of "soft spots," such as impurities and dislocations, may lower the binding forces surrounding the recoil atom, thus allowing displacements at smaller or subthreshold energies. This effect may also be due to displacement of impurities themselves (ref. 3). Considering the apparently strong effects of impurities on defect recovery in tungsten (refs. 21 and 22) and the fact that tungsten's threshold is probably greater than that of any impurity it contains, one would tend to attribute the 4 K lowest data point to impurity-related subthreshold displacements. Nonetheless, whatever its source, this type of low energy damage recovers somewhere between 4 and 350 K since it was not observed in the results of figure 2.

Fundamental Aspects

Having established a bare outline of the temperature dependence of threshold in tungsten, let us consider what fundamental knowledge might be deduced by comparing the data of table II with displacement and recovery theory (see Theoretical Effects of Temperature section).

Because the damage retained during a Stage II irradiation of tungsten and other metals can be attributed to equal concentrations of impurity-trapped FIA and vacancies, it follows that $E_d^o(350\ K) = 50\pm2$ eV is the minimum recoil energy required for FIA production at 350 K. Although the exact contribution of TEDE to this onset is unknown, the value of 50±2 eV should be the onset threshold measured at any Stage II temperature (100 to 600 K). This conclusion is based on the fact that damage retention anywhere within Stage II requires FIA production and that the only perturbation to onset is TEDE which changes insignificantly across Stage II (from -3 to -6 eV).

To estimate interstitial thresholds in a tungsten lattice free of thermal vibration, one can employ equation (10) to find

$$E_d(FIA) = 53\pm5\ eV \tag{11}$$

If it is assumed that the 4 K onset measured by Neely, Keefer, and Sosin was not caused by extrinsic sources, then 40±2 eV equals $E_d^o(0\ K)$, the threshold for the production of a close Frenkel pair with minimum interstitial-vacancy separation. Thus,

$$\Delta E_{FIA} = 13\pm7\ eV \tag{12}$$

is the extra recoil energy required above $E_d^o(0\ K)$ to deposit a tungsten interstitial in a lattice position at which its motion is unaffected by its own vacancy. This energy difference would be even smaller if $E_d^o(4\ K)$ were due to subthreshold displacements. For if this were the case, one might then assume $E_d^o(0\ K) \cong E_d^o(35\ K)$ (neglecting TEDE and the retention problem) to find $\Delta E_{FIA} = 6\pm8$ eV.

Although only polycrystalline specimens were employed in the present study, general information concerning $E_d\langle hk\ell\rangle$ for tungsten may be obtained by comparing the above results with the computer calculations on bcc iron (ref. 16). For instance, let us assume that the following directional results of this latter study are also applicable to bcc tungsten:

(1) $E_d^o(0\ K) = E_d\langle 100\rangle \leq E_d\langle hk\ell\rangle$; that is, near 0 K the first observable damage is produced by atoms which have recoiled in the $\langle 100\rangle$ directions.

(2) $E_d\langle 111\rangle \geq E_d\langle hk\ell\rangle$; that is, neglecting a few low probability recoil directions, atoms recoiling in the $\langle 111\rangle$ directions require the largest recoil energy to produce an interstitial.

(3) $E_d(\text{FIA}) \geq E_d\langle 111\rangle$; that is, replacement collision chains in the close-packed $\langle 111\rangle$ directions are the most probable source of FIA.

Applying the previously mentioned iron results to the data of table II, one obtains

$$\left.\begin{aligned} E_d\langle 100\rangle &= 40\pm2 \text{ eV} \leq E_d\langle hk\ell\rangle \\ \text{and} \\ E_d\langle hk\ell\rangle &\leq E_d\langle 111\rangle \leq 53\pm5 \text{ eV} \end{aligned}\right\} \quad (13)$$

indicating threshold energy in tungsten does not vary significantly with recoil direction. This variation would even be less if $E_d^o(4\text{ K})$ were caused by subthreshold displacements. Approximate threshold isotropy is also suggested by the fact that one effective threshold fits the commercial data of figure 2 at all energies. If FIA threshold varied appreciably with recoil direction, E_d^* over any small energy interval would not be independent of electron energy but would increase monotonically as more directions for FIA displacement became active.

The indication of approximate threshold isotropy in tungsten is in opposition to the theoretical estimates of Andersen and Sigmund (ref. 26) who calculate $E_d\langle 111\rangle = 2.4\ E_d\langle 100\rangle$. Admittedly the directional dependence of E_d is best determined with single crystals where directional measurements are more straightforward and are not subjected to the uncertainties contained in the association of certain defect types with certain crystal directions. Nonetheless, the previous analysis does suggest that $E_d\langle hk\ell\rangle$ in tungsten is more isotropic than the calculations of Andersen and Sigmund would seem to indicate.

DAMAGE PRODUCTION ABOVE THRESHOLD

According to low dose Stage II theory (eq. (5)), the energy dependence of the 350 K damage rate is produced by two factors: $f(\epsilon)$ and $\sigma_d(\epsilon, E_d^*)$. Since E_d^* has been shown to be temperature independent, it follows from equation (3) that σ_d has the same energy dependence as the damage rate near 4 K. Thus $f(\epsilon)$, the FIA fraction of the total interstitial concentration, is directly proportional to the ratio of the 350 K to the 4 K rates. Explicity from equations (3) and (5),

$$f(\epsilon) = \left[\frac{\rho_F}{\rho^*}\right] \left[\frac{\left(\frac{d\rho}{d\Phi}\right)_{350\ K}}{\left(\frac{d\rho}{d\Phi}\right)_{4\ K}}\right] \tag{14}$$

Applying this equation with $\rho^* = \rho_F$ to the data of figure 3 and the commercial results of figure 2, one can then determine the energy dependence of $f(\epsilon)$. For instance, at 1.6 MeV, f = 0; at 1.9 MeV, f = 0.22; and at 2.4 MeV, f is 0.33 or less depending on whether E_d^* is 46 eV or greater. Thus, as energy increases above threshold, $f(\epsilon)$ rises rapidly from zero and then tends to level off. Since f is the fraction of FIA, it follows that after a low temperature irradiation the percentage of Stage I recovery due to FIA should also show a tendency to saturate with increasing energy. Energy dependence such as this has already been observed for FIA recovery in some fcc metals (ref. 27).

The 350 K damage rate results indicate that f may also depend on impurity concentration. Assuming that the commercial (C) and high purity (HP) specimens have the same σ_d and ρ^*, then one finds from low dose theory (eq. (5)) and figure 2 that $f_{HP}/f_C \cong 0.5$. Because neither specimen type should have contained enough impurities to affect the displacement process above threshold (ref. 3), this purity effect must be related to the process of FIA retention. Accepting this, the simplest interpretation which can then be invoked is that there is a higher probability with larger impurity concentration that some CPIA will be created within the capture radii of the impurities. Upon creation in Stage II these CPIA are immediately attracted away from their own vacancies by the impurities and thereby counted as trapped FIA. This mechanism is consistent with observed impurity effects in copper (ref. 28) where close-pair recovery in Stage I has been measurably reduced by large impurity concentrations. However, even though this CPIA capture mechanism is a reasonable interpretation, there are at least two other possible sources for the purity effects. These are based on the possibility that the inequality in damage rates for the two specimen types was produced totally, or in part, by the parameter ρ^*. For instance, due to a difference in impurity types the resistivity of a trapped interstitial in the pure specimen may be smaller than that in the commercial specimens. Or, because defect resistivity was measured at 291 K, deviations from Mathiessen's rule may exist, causing $\rho_C^* > \rho_{HP}^*$. Nevertheless, whatever the source, it is apparent that in the low dose region resistance ratios ranging from 10 to 1000 produce only a small effect on Stage II damage rates.

Finally, to determine the energy dependence of low dose Stage II defect production in tungsten, one can employ the following relation which adequately describes the results of figure 2:

$$\left[\frac{d\rho}{d\Phi}(\epsilon)\right]_{II} = f_o\rho^* \sigma_d(\epsilon, 52\ \text{eV}) \tag{15}$$

where the product $f_o\rho^*$ is a constant. If the energy dependence of f is averaged from 1.9 to 2.4 MeV, then equation (15) gives $f_C = 0.28\pm0.06$ and $f_{HP} = 0.14\pm0.03$. Here it is assumed that $46\ \text{eV} \leq E_d^* \leq 52\ \text{eV}$, $\rho^* = \rho_F$, and Mathiessen's rule holds at 291 K. Thus in the low dose region

$$\left[\frac{dN_F}{d\Phi}(\epsilon)\right]_{II} = \frac{1}{\rho^*}\left[\frac{d\rho}{d\Phi}(\epsilon)\right]_{II} = (0.22\pm0.12)\sigma_d(\epsilon, 52\ \text{eV}) \tag{16}$$

where N_F is the electron-induced Frenkel pair concentration created near 350 K in polycrystalline tungsten of any practical purity. If variations in ρ^* are neglected, the contents of the section Theoretical Effects of Temperature predict that equation (16) should hold across all of Stage II, that is, 100 to 600 K. Further experimentation within this temperature range should test this prediction.

THRESHOLD IN bcc TRANSITION METALS

The near isotropy of $E_d\langle hk\ell\rangle$ in elastically isotropic tungsten suggests that perhaps some correlation exists between threshold energy and directionally dependent elastic properties. Although there seems to be no a priori reason why such a relation should exist, it was of interest to check whether similar behavior could be found in other bcc transition metals. Lucasson and Walker (ref. 29) who electron-irradiated both polycrystalline iron and molybdenum specimens near 20 K found that E_d^* for iron was not well-defined; that is, the energy-dependent data could not be fit to a simple step-function probability of displacement but required a function which rose from zero to unity over a wide range of recoil energies. Erginsoy, Vineyard, and Englert (ref. 16) subsequently showed that this requirement of a nonsimple probability function could be explained by anistropy in iron's $E_d\langle hk\ell\rangle$. Regarding molybdenum, however, Lucasson and Walker found that a simple step-function displacement probability could fit all the data, even those damage rate points close to zero. Thus by comparison with the iron it appears that threshold for molybdenum is isotropic; that is, $E_d\langle hk\ell\rangle \cong E_d^*$. Because iron and molybdenum are elastically anisotropic and isotropic, respectively, the results of Lucasson and Walker seem to qualitatively support a correlation between the directional dependence of threshold energy and elasticity. Encouraged by this we have examined whether any general quantitative agreement could be found among the three bcc metals for which thresholds have been measured.

An elastic property which like threshold depends on crystal direction is Young's modulus Y. For the stress direction $\langle hk\ell \rangle$ in a cubic crystal with elastic constants C_{11}, C_{12}, and C_{44}, Y is given by (ref. 30)

$$(Y\langle hk\ell \rangle)^{-1} = (Y\langle 100 \rangle)^{-1} - (A - 1)\,\Gamma(C_{44})^{-1} \tag{17}$$

Here A, the anisotropy factor, equals $2C_{44}/(C_{11} - C_{12})$;

$$Y\langle 100 \rangle = \frac{(C_{11} - C_{12})(C_{11} + 2C_{12})}{(C_{11} + C_{12})} \tag{18}$$

and Γ, the orientation factor, is expressed in terms of the direction cosines γ_1, γ_2, and γ_3 of the stress direction relative to the three cube axes

$$\Gamma = \gamma_1^2\gamma_2^2 + \gamma_2^2\gamma_3^2 + \gamma_3^2\gamma_1^2 \tag{19}$$

An anisotropy factor of unity indicates elastic isotropy, that is, $Y\langle hk\ell \rangle = Y\langle 100 \rangle$. Using the appropriate low temperature elastic constants (ref. 31), we calculated $Y\langle 100 \rangle$ ($\Gamma = 0$) and $Y\langle 111 \rangle$ ($\Gamma = 1/3$) for a number of bcc transition metals. The results are given in table III Also included are the available experimental E_d^o for each metal plus the computer-calculated $E_d\langle hk\ell \rangle$ for iron (ref 16). The uncertainty in $E_d\langle 100 \rangle$ for tungsten arises from the possibility that subthreshold displacements may have influenced this measurement. Comparing the experimental E_d^o with the minimum $Y\langle hk\ell \rangle$ we find

$$\frac{E_d^o}{Y_{min}} \cong 1.2\times10^{-6}\ (eV)(cm^2)/N \cong 20\ \text{Å}^3 \tag{20}$$

Assuming this threshold to modulus ratio holds for all bcc transition metals and all crystal directions, we can then predict $E_d\langle hk\ell \rangle$ from $Y\langle hk\ell \rangle$. These empirical predictions are given in the second last column of table III. Finally, the last column indicates the Andersen and Sigmund (ref. 26) theoretical estimates of $E_d\langle hk\ell \rangle$ for each metal.

From table III it can be seen that wherever experimental or computer-calculated bcc thresholds are available, fairly good quantitative agreement is achieved by assuming $E_d\langle hk\ell \rangle$ directly proportional to $Y\langle hk\ell \rangle$ through the equation (20) constant. It is also clear that this type of empirical correlation is more useful than the predictions employed by Andersen and Sigmund. These authors assumed that each bcc $E_d\langle hk\ell \rangle$ is proportional to the value of the interatomic potential at an atomic separation equal to the nearest neighbor distance along the $\langle hk\ell \rangle$ direction. Their directionally dependent proportionality constants were obtained from the computer results on iron; whereas their

interatomic potentials were assumed to be Born-Mayer, that is, $A_o \exp(-r/a_o)$. Regarding the parameters a_o and A_o, they found that good agreement with the threshold results of fcc copper, silver, and gold could be achieved by assuming a_o is a constant and A_o is proportional to the 3/2 power of the atomic number. From table III it is apparent that this choice of parameters for the bcc transition metals is not as universal as Andersen and Sigmund assumed.

Although reasons for the apparent success of threshold-modulus correlation are far from obvious, perhaps the following argument may shed some light. In general, application of correlation with one proportionality constant to the fcc metals has proven to be less successful than the method of Andersen and Sigmund. One possible exception is nickel which, although it possesses an fcc structure, is a transition metal. This suggests that the unfilled d-shells are the source of threshold-modulus correlation. In any metal, threshold should be the energy required to force the outer shells of the struck atom through the outer shells of its nearest neighbors. In the transition metals, cohesive energy and thus Young's modulus are due primarily to the local interaction of the unfilled d-shells. However, in the nontransition metals such as the noble metals, cohesive energy and modulus are due to the nonlocal long range interactions of the valence electrons. Therefore, threshold-modulus correlation might be expected in the transition metals but not in the noble metals. This possibly might also explain why the Born-Mayer constants derived by Andersen and Sigmund from the noble metals do not apply as well to the bcc transition metals. Suffice to say, the correlation method like the Andersen-Sigmund method is based on only three metals so that future bcc threshold measurements may totally nullify its general usefulness. Regarding this point it appears that a good test metal would be chromium since the E_d^o prediction by modulus correlation (31 eV) is noticeably different than that given by Andersen and Sigmund (12 eV).

CONCLUSIONS

The present study has measured the energy dependence of the rate at which electron-induced radiation damage accumulates in commercial and high purity tungsten near 350 K. From these results the minimum or threshold energy for the onset of observable damage was determined to be 1.62±0.04 MeV, or, in terms of atomic recoil energy, E_d^o = 50±2 eV. An "effective" threshold of 52±2 eV was also determined by directly comparing the energy dependence of the damage rates to the energy dependence of the "best fit" theoretical cross section calculated from a step-function displacement probability.

The aforementioned results in combination with low temperature damage rate data, bcc displacement theory, and the accepted mechanisms for defect recovery leads one to the following conclusions:

1. Since the irradiations were performed at temperatures within Stage II recovery, the observed damage consisted primarily of equal concentrations of vacancies and impurity-trapped interstitials. In order to reach impurities, these interstitials were initially created at lattice positions from which they could migrate freely, that is, unaffected by their own vacancies. Thus the onset threshold result of 50±2 eV is attributed to the minimum recoil energy required to produce an uncorrelated or "free" interstitial atom (FIA) in tungsten near 350 K. Because the effect of thermal vibrations varies insignificantly across Stage II, 50±2 eV should be the onset threshold measured anywhere from 100 to 600 K.

2. From a re-examination of previously published low temperature damage rates, the effective threshold near 4 K was determined to be 46 eV or greater. This result suggests that the 4 K onset of 40±2 eV measured by Neely, Keefer, and Sosin may have been caused by impurity-related subthreshold displacements.

3. For a tungsten lattice free of thermal vibration, the minimum recoil energy to create an FIA is 53±5 eV. Comparison of this result with $E_d^o(4\ K)$ indicates that the extra recoil energy $\Delta E_{FIA} = 13\pm7$ eV is required to increase the minimum interstitial-vacancy separation to the point where the interstitial is uncorrelated or unaffected by the vacancy. If subthreshold events did affect the measured 4 K onset, this energy difference is even smaller, that is, $\Delta E_{FIA} \cong 6\pm8$ eV. By assuming that the qualitative computer findings on bcc iron apply also to bcc tungsten, it can be shown that the variation in $E_d\langle hk\ell\rangle$ with recoil direction is no greater than ΔE_{FIA}. Thus threshold in tungsten is nearly isotropic.

4. A difference of two orders of magnitude in impurity content was found to have only a small effect on low dose damage rates. Consequently, an equation is derived for estimating the Stage II energy dependence of Frenkel pair production in tungsten of any practical purity. This result, however, is limited to low doses and recoil energies below ~100 eV.

5. Finally, the finding of approximate threshold isotropy in elastically isotropic tungsten has suggested a possible correlation in bcc transition metals between the recoil direction dependence of threshold energy ($E_d\langle hk\ell\rangle$) and the directional dependence of Young's modulus ($Y\langle hk\ell\rangle$). Indeed, it is shown that both qualitative and quantitative evidence exist for such correlation in iron and molybdenum, the only other bcc metals for which threshold has been determined. The low temperature directionally dependent threshold energies of iron, molybdenum, tungsten, niobium, chromium, tantalum, and vanadium are calculated using the relation $E_d\langle hk\ell\rangle / Y\langle hk\ell\rangle = 1.2\times10^{-6}$ (eV)(cm^2)/N. These results are compared with the theoretical predictions of Andersen and Sigmund.

Wherever experimental data exist, significantly better agreement is found for the correlation method. Only further experimental and theoretical studies of bcc thresholds will determine the general usefulness of the modulus-correlation approach.

Lewis Research Center,
National Aeronautics and Space Administration,
Cleveland, Ohio, June 3, 1971,
129-03.

REFERENCES

1. Thompson, M. W.: The Damage and Recovery of Neutron Irradiated Tungsten. Phil. Mag., vol. 5, no. 51, Mar. 1960, pp. 278-296.

2. DiCarlo, J. A.; and Townsend, J. R.: Internal Friction Peaks in Deuteron-Irradiated Tungsten. Acta Met., vol. 14, no. 12, Dec. 1966, pp. 1715-1722.

3. Sosin, A.; and Bauer, W.: Atomic Displacement Mechanism in Metals and Semiconductors. Studies in Radiation Effects in Solids. Vol. 3. George J. Dienes, ed., Gordon and Breach Science Publ., 1969, pp. 153-327.

4. Neely, H. H.; and Sosin, A.: Electron Irradiation of Copper and Aluminum above Stage I. Phys. Rev., vol. 152, no. 2, Dec. 9, 1966, pp. 623-628.

5. Evans, J. H.: A Quantitative Study of the Dose and Impurity Dependence of the Defect Concentrations Remaining in Molybdenum after 4 MeV Electron Irradiation at (77° K). Acta Met., vol. 18, no. 5, May 1970, pp. 499-504.

6. Walker, R. M.: Electron-Induced Radiation Damage in Pure Metals. Radiation Damage in Solids. D. S. Billington, ed., Academic Press, 1962, pp. 594-629.

7. Schultz, H.: Die Erholung Des Elektrischen Widerstandes Von Kaltverformtem Wolfram. Acta Met., vol. 12, no. 5, May 1964, pp. 649-664.

8. DiCarlo, J. A.; Snead, C. L., Jr.; and Goland, A. N.: Stage-I Interstitials in Electron-Irradiated Tungsten. Phys. Rev., vol. 178, no. 3, Feb. 15, 1969, pp. 1059-1072.

9. Stevenson, F. R.; and Gauntner, D. J.: Characteristics of Composite Carbon Resistors Used for Measuring Accelerator Terminal Voltages. Rev. Sci. Instr., vol. 40, no. 1, Jan. 1969, pp. 140-144.

10. Sosin, A.: Energy Dependence of Electron Damage in Copper. Phys. Rev., vol. 126, no. 5, June 1, 1962, pp. 1698-1710.

11. Berger, Martin J.; and Seltzer, Stephen M.: Tables of Energy Losses and Ranges of Electrons and Positrons. NASA SP-3012, 1964.

12. Oen, O. S.: Displacement Cross Sections by Fast Electrons. Radiation Effects in Semiconductors. Frederick L. Vook, ed., Plenum Press, 1968, pp. 264-279.

13. Bethe, H. A.: Molière's Theory of Multiple Scattering. Phys. Rev., vol. 89, no. 6, Mar. 15, 1953, pp. 1256-1266.

14. Burke, Edward A.; Grossbard, Niel J.; and Lowe, Lester F.: Calculated Cross Sections for Atomic Displacements Produced by Electrons in the 1.0-3.0 MeV Energy Range. Rep. AFCRL-65-286, Air Force Cambridge Research Labs., Apr. 1965. (Available from DDC as AD-616245.)

15. Gibson, J. B.; Goland, A. N.; Milgram, M.; and Vineyard, G. H.: Dynamics of Radiation Damage. Phys. Rev., vol. 120, no. 4, Nov. 15, 1960, pp. 1229-1253.

16. Erginsoy, C.; Vineyard, G. H.; and Englert, A.: Dynamics of Radiation Damage in a Body-Centered Cubic Lattice. Phys. Rev., vol. 133, no. 2A, Jan. 20, 1964, pp. 595-606.

17. Corbett, James W.: Electron Radiation Damage in Semiconductors and Metals. Academic Press, 1966.

18. Kinchin, G. H.; and Thompson, M. W.: Irradiation Damage and Recovery in Molybdenum and Tungsten. J. Nucl. Energy, vol. 6, no. 4, 1958, pp. 275-284.

19. Coltman, R. R.; Klabunde, C. E.; and Redman, J. K.: Survey of Thermal-Neutron Damage in Pure Metals. Phys. Rev., vol. 156, no. 3, Apr. 15, 1967, pp. 715-734.

20. Neely, H. H.; Keefer, D. W.; and Sosin, A.: Electron Irradiation and Recovery of Tungsten. Phys. Stat. Sol., vol. 28, 1968, pp. 675-682.

21. Scanlan, R. M.; Styris, D. L.; and Seidman, D. N.: An In-situ Field Ion Microscope Study of Irradiated Tungsten. I. Experimental Results. Rep. 1340, Cornell Univ. Materials Sci. Center, 1970. (Work under contract AT30-1-3504.) To be published in Phil. Mag.

22. Scanlan, R. M.; Styris, D. L.; and Seidman, D. N.: An In-situ Field Ion Microscope Study of Irradiated Tungsten. II. Analysis and Interpretation. Rep. 1385, Cornell Univ. Materials Sci. Center, 1970. (Work under contract AT30-1-3504.) To be published in Phil. Mag.

23. Johnson, R. A.: Interstitials and Vacancies in α Iron. Phys. Rev., vol. 134, no. 5, June 1, 1964, pp. 1329-1336.

24. Nihoul, J.: Vacancies and Interstitials in Body-Centred Cubic Metals. Vacancies and Interstitials in Metals. A. Seeger, D. Schumacher, W. Schilling, and J. Diehl, eds., North-Holland Publ. Co., 1970, pp. 839-888.

25. Roberts, Clyde G.: Low Temperature Recovery of Electron-Irradiated Tungsten. Ph. D. Thesis, Univ. North Carolina, 1968.

26. Andersen, H. H.; and Sigmund, P.: On the Determination of Interatomic Potentials in Metals by Electron Irradiation Experiments. Rep. R1S0-103, Danish Atomic Energy Commission Research Establishment, May 1965.

27. Chaplin, R. L.; and Simpson, H. M.: Energy Dependence of the Stage-I Recovery of Aluminum. Phys. Rev., vol. 163, no. 3, Nov. 15, 1967, pp. 587-591.

28. Sosin, A.; and Neely, H. H.: Influence of Foreign Solute Atoms on Stage I Recovery in Electron-Irradiated Copper. Phys. Rev., vol. 127, no. 5, Sept. 1, 1962, pp. 1465-1470.

29. Lucasson, P. G.; and Walker, R. M.: Production and Recovery of Electron-Induced Radiation Damage in a Number of Metals. Phys. Rev., vol. 127, no. 2, July 15, 1962, pp. 485-500.

30. Berry, B. S.; and Nowick, A. S.: Anelasticity and Internal Friction Due to Point Defects in Crystals. Effect of Imperfections. Vol. III, Part A of Physical Acoustics: Principles and Methods. Warren P. Mason, ed., Academic Press, 1966, p. 10.

31. Leibfried, G.: The Vibrational Frequency Spectrum of Some Body-Centered Cubic Metals. Diffusion in Body-Centered Cubic Metals. American Society for Metals, 1965, p. 115.

TABLE I. - ENERGY DEPENDENCE OF DAMAGE RATE NEAR 350 K

Specimen	Incident electron energy, ϵ_i, MeV	Maximum recoil energy, E_r^{max}, eV	Damage rate, $(d\rho/d\Phi)_m$, ohm-cm/electrons/cm^2
Commercial purity 1	2.30±0.01	89	[a](7.83±0.39)×10^{-27}
Commercial purity 2	1.70±0.01	54	(0.34±0.04)×10^{-27}
	1.90	65	(1.40±0.14)
	2.10	77	(4.00±0.15)
	2.20	83	(5.22±0.14)
Commercial purity 3	1.59±0.01	49	(0.00±0.01)×10^{-27}
	1.85	62	(0.92±0.03)
	2.00	71	(2.69±0.04)
	2.25	86	(5.68±0.11)
	2.40	96	(8.11±0.01)
High purity 1	2.10±0.01	77	(1.59±0.03)×10^{-27}
	2.40	96	(4.52±0.24)

[a]No temperature controller.

TABLE II. - TEMPERATURE DEPENDENCE OF THRESHOLD ENERGY IN TUNGSTEN

Threshold energy	Stage I (~4 K)	Stage I (~35 K)	Stage II (~350 K)
Threshold for onset of damage, E_d^o, eV	[a]40±2	[b]47±3	[c]50±2
Effective threshold, E_d^*, eV	[d]≥46	-----	[e]52±2

[a]Ref. 20.
[b]Ref. 25.
[c]Present study.
[d]From combination of refs. 20 and 8; see text and fig. 3.
[e]Present study under assumption $f(\epsilon)$ = constant.

TABLE III. - COMPARISON OF THRESHOLD ENERGIES IN bcc TRANSITION METALS

Metal	Crystal direction, $\langle hk\ell \rangle$	Young's modulus (experimental)[a], $Y\langle hk\ell \rangle$, N/cm^2	Threshold energy, $E_d\langle hk\ell \rangle$, eV		
			Experimental (approximate)	Theoretical	
				Present study	Andersen-Sigmund[b]
Iron	$\langle 100 \rangle$	14×10^6	[c]17	17	14
	$\langle 110 \rangle$	23	[d]34	28	--
	$\langle 111 \rangle$	29	[d]38	35	31
Molybdenum	$\langle 111 \rangle$	32×10^6	[e]37	38	35
	$\langle 100 \rangle$	35	[e]37	42	15
Tungsten	$\langle 100 \rangle$	42×10^6	[f]40 to 47	50	34
	$\langle 111 \rangle$	42	[g]53	50	80
Niobium	$\langle 111 \rangle$	8×10^6	---	10	26
	$\langle 100 \rangle$	15	---	18	11
Chromium	$\langle 111 \rangle$	26×10^6	---	31	26
	$\langle 100 \rangle$	36	---	43	12
Tantalum	$\langle 100 \rangle$	15×10^6	---	18	25
	$\langle 111 \rangle$	23	---	28	61
Vanadium	$\langle 111 \rangle$	13×10^6	---	15	--
	$\langle 100 \rangle$	15	---	18	--

[a]From eqs. (17) - (19), and ref. 31.
[b]Ref. 26.
[c]Ref. 3.
[d]Computer-calculated results from ref. 16.
[e]Deduced from ref. 29; see text.
[f]Refs. 20 and 25.
[g]Present study.

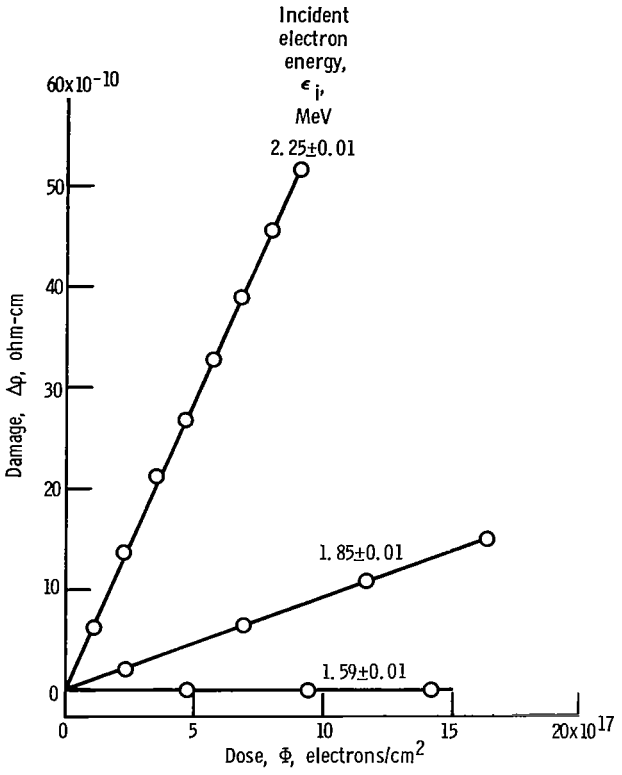

Figure 1. - Typical damage production curves for low dose irradiations near 350 K. Commercial purity specimen 3.

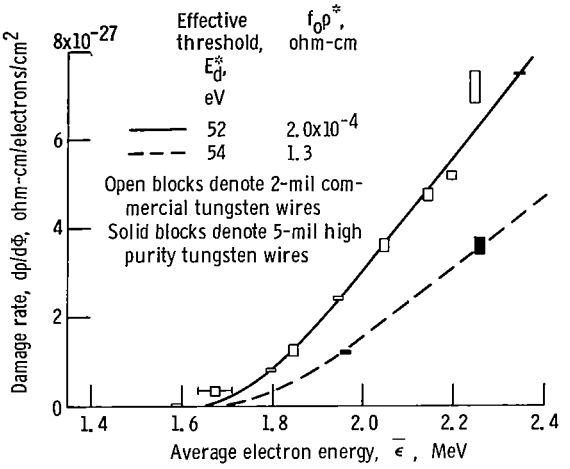

Figure 2. - Damage rate near 350 K plotted against average electron energy for 2-mil commercial and 5-mil high purity tungsten wires. All data have been corrected for path length (eqs. (7) and (8)).

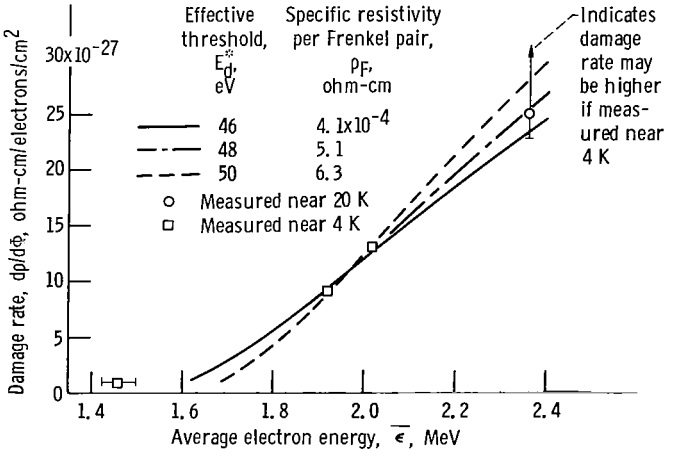

Figure 3. - Damage rate near 4 K plotted against average electron energy as measured by Neely, Keefer, and Sosin (ref. 20) with 3-mil tungsten wires. Damage rate near 20 K measured by DiCarlo, Snead, and Goland (ref. 8) with 5-mil wire is also included for comparison. All data have been corrected for path length (eqs. (7) and (8)).

"The aeronautical and space activities of the United States shall be conducted so as to contribute . . . to the expansion of human knowledge of phenomena in the atmosphere and space. The Administration shall provide for the widest practicable and appropriate dissemination of information concerning its activities and the results thereof."

—NATIONAL AERONAUTICS AND SPACE ACT OF 1958

NASA SCIENTIFIC AND TECHNICAL PUBLICATIONS

TECHNICAL REPORTS: Scientific and technical information considered important, complete, and a lasting contribution to existing knowledge.

TECHNICAL NOTES: Information less broad in scope but nevertheless of importance as a contribution to existing knowledge.

TECHNICAL MEMORANDUMS: Information receiving limited distribution because of preliminary data, security classification, or other reasons.

CONTRACTOR REPORTS: Scientific and technical information generated under a NASA contract or grant and considered an important contribution to existing knowledge.

TECHNICAL TRANSLATIONS: Information published in a foreign language considered to merit NASA distribution in English.

SPECIAL PUBLICATIONS: Information derived from or of value to NASA activities. Publications include conference proceedings, monographs, data compilations, handbooks, sourcebooks, and special bibliographies.

TECHNOLOGY UTILIZATION PUBLICATIONS: Information on technology used by NASA that may be of particular interest in commercial and other non-aerospace applications. Publications include Tech Briefs, Technology Utilization Reports and Technology Surveys.

Details on the availability of these publications may be obtained from:

SCIENTIFIC AND TECHNICAL INFORMATION OFFICE

NATIONAL AERONAUTICS AND SPACE ADMINISTRATION

Washington, D.C. 20546